

PIV Measurement of Flow-Patterns in a Human Vocal Tract Model

J. Horáček¹, P. Šidlof, V. Uruba, J. Veselý, V. Radolf, V. Bula

Institute of Thermomechanics, Academy of Sciences of the Czech Republic, ¹Email: jaromirh@it.cas.cz

Introduction

Voice production is a complex physiological process, which involves several basic factors like airflow coming from the lungs, vocal-folds vibration and acoustic resonances of the cavities of the human vocal tract [1].

There are problems with investigation of the airflow pattern in the glottis region *in vivo*. Thus the measurements of the flow characteristics and regimes are provided on various physical models. Several experiments were performed for flows in “2D” rigid *in vitro* models of the glottis [2,3], where mainly static pressure measurements were carried out for different geometries of the glottal region. Such experiments concentrated on the effects of the channel asymmetry and shape (convergent, liplike, divergent). Later, similar studies were provided with vibrating replicas of the vocal folds [4,5]. Recently, Particle Image Velocimetry (PIV) technique enabled new possibilities in such studies [6-8].

This study describes developed complex physical model of the voice production that consists of the trachea, the self-oscillating vocal folds and the vocal tract with acoustical spaces corresponding to the vowel /a:/. The time-resolved PIV method was used for instantaneous velocity field evaluation. The vibrating vocal folds during oscillation were recorded by the high-speed camera in the same instants as the airflow velocity patterns. The results are presented for measurements performed within a physiologically range of mean airflow rates and fundamental frequencies.

Measurement set-up

The schema of the all instrumentation and of the test rig is shown in Figure 1. The airflow was coming from a pressure vessel (PV-17) joint to a central compressor. Prior to the measurement, the storage tank (ST-2) was filled with the smoke particles coming from the generator (GEN-1). Then the corresponding valve was closed. The mean airflow rate in the main measurement line was controlled by the digital (DFC-3 and PC1-4) and the float (FM-20) flow meters. Before entering the glottal region of the model with the mounted vocal folds (VF-6) the subglottal pressure in the model of the trachea (SUB-18) was measured by semiconductor pressure transducers (PT-5) mounted on the channel wall. The PIV laser sheet (LAS-PIV-7) was focused on a part of the vocal tract model (VT-19), which was observed by the PIV high-speed camera (CAM-PIV-11). The self-oscillating vocal folds were synchronously recorded by the second high-speed PIV camera (CAM-IM-12). The microphone of the sound level meter (B&K SLM-13) was installed in the distance of 30 cm from the outlet of the vocal tract 2D model. The time signals from the pressure transducers and microphone were measured by the B&K measurement system (PULSE-14) controlled by a computer

(PC-15). The main computer (PC3-16) controlled the complete PIV system and the computer (PC4-21) was used for recording the vocal folds model vibrations.

Vocal tract model

A simplified “2D” plexiglass model of the vocal tract was developed from the 3D FE models designed from MR images [9]. To ensure their correspondence, the “1D” and “3D” models have the same areas in the cross-sections along the vocal tract. This “2D” with another two plane-parallel walls enabled to use the Particle Image Velocimetry (PIV) method for the airflow investigation. The shape of the “2D” vocal tract model for the vowel /a:/ is sketched in Figure 2.

Vocal folds model

The shape and dimensions of the vocal folds model are shown in Figure 3. The vocal folds skin was made of a latex thin cover layer filled by a compound prepared from polyurethane elastomer VytaFlexTM consisted of parts A and B and the softener So-Flex mixed in the ratio 1:1:3. The vocal fold model was joined to the model of the subglottal spaces made of a plexiglass tube (260 mm length, 26 mm inner diameter).

PIV system

The time-resolved PIV method was used for instantaneous velocity field evaluation. The measuring system DANTEC consists of laser New Wave Pegasus (Nd:YLF, cylindrical optics, double head, wavelength 527 nm, frequency up to 10 kHz, shot energy 10 mJ for 1 kHz) and CCD camera NanoSense MkIII with maximal resolution 1280x1024 pixels and corresponding maximal frequency 512 double-frames per second. The camera memory 4 GB represents 1635 full resolution double-frames. The maximal frequency of the camera is limited by data rate, so it could be augmented by reducing the resolution. In the experiments, we used reduced resolution with maximal possible frequency and 1000 consecutive snapshots were acquired. As tracing particles the cigarette smoke was used. The software Dynamics Studio ver. 2 was used for both data acquisition and velocity-fields evaluation by application of the adaptive correlation method.

Results

The results are presented here for the measurement No 57 with the mean airflow rate $Q_{\text{mean}}=0.25$ l/s, fundamental frequency of the vocal folds self-oscillation $F_0=158$ Hz, time difference between the two laser-pulses $\Delta t=6$ μ s and the laser frequency $f_{\text{las}}=1582$ Hz.

The microphone and subglottal pressure signals are shown in Figure 4 together with the glottal gap width in the vocal folds cross-section where the PIV measurement was performed.

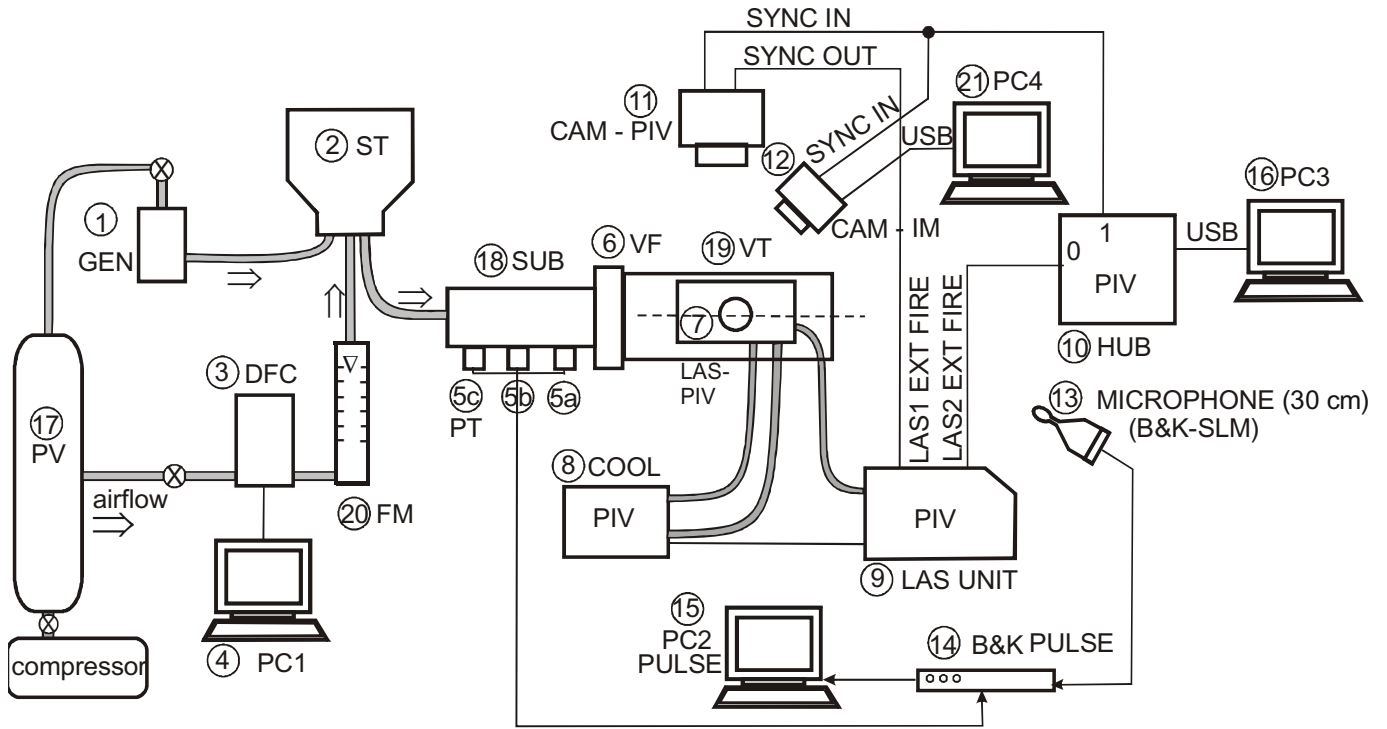


Figure 1: Schema of the measurement set-up.

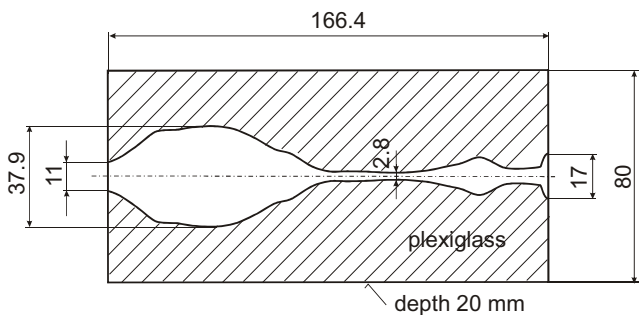


Figure 2: Schema of the vocal tract model - vowel /a:/.
plexiglass
depth 20 mm

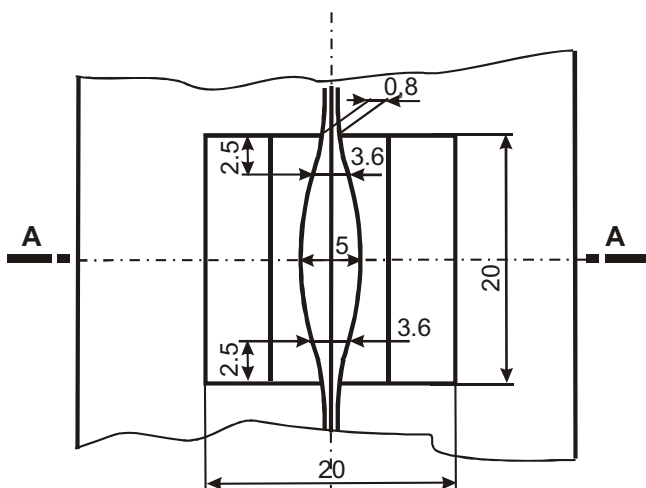


Figure 3: Schema of the vocal folds model mounted in a supporting frame.

The signals are not perfectly periodic, because the vocal fold vibrations were not exactly repeatable in each oscillation cycle and the sampling frequency was not sufficient due to the limits of the PIV system.

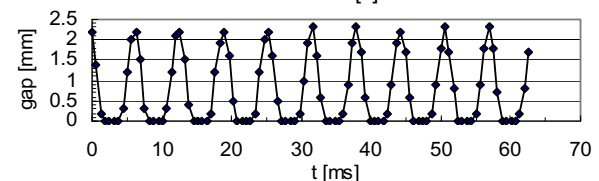
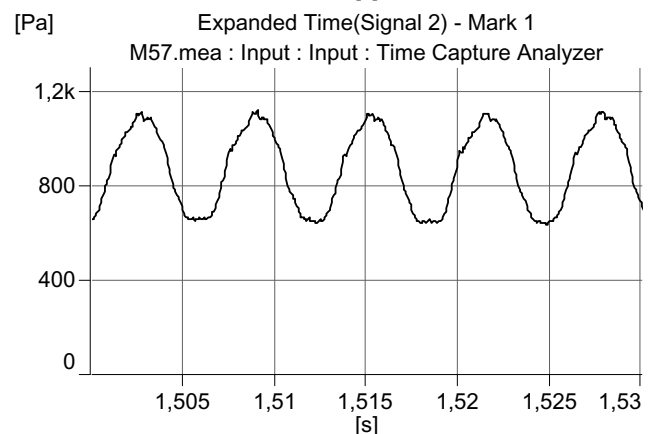
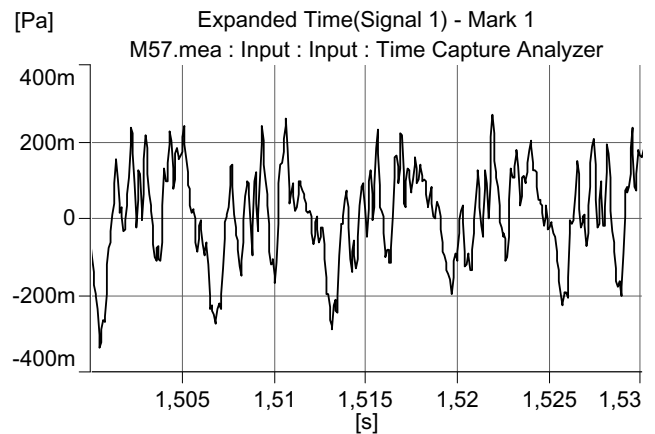


Figure 4: Microphone signal (radiated sound from the vocal tract), subglottal pressure measured by the pressure transducer in the model of the trachea and the glottal gap.

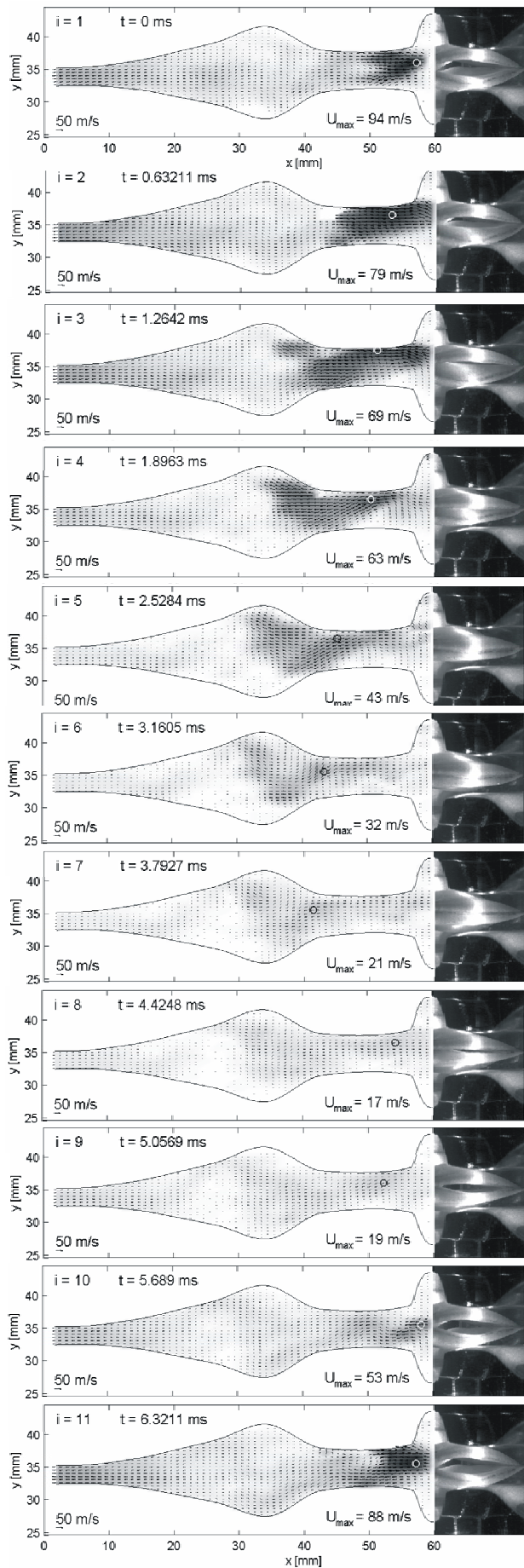


Figure 5: Airflow velocities measured near the glottal region and vibration of the vocal folds model in $i=1-11$ time instants during 1st oscillation cycle. (The air flows from the right to the left.)

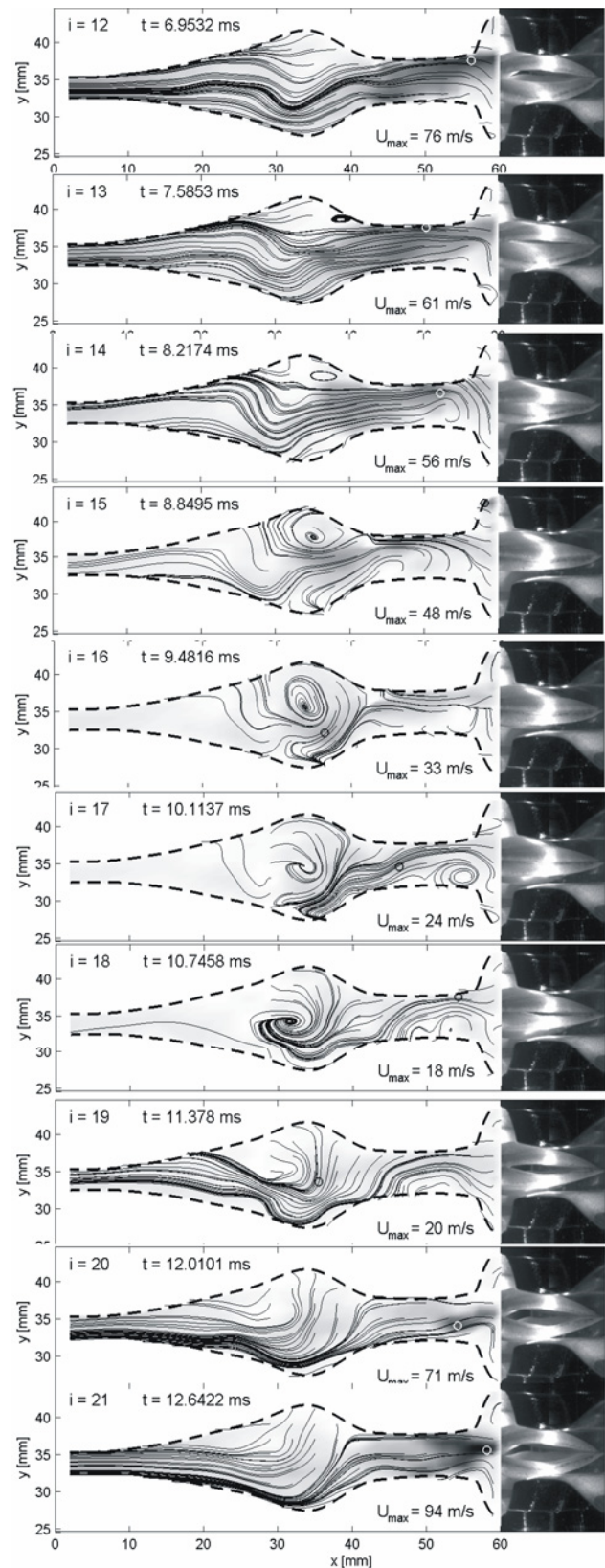


Figure 6: Streamlines measured near the glottal region and vibration of the vocal folds model in $i=12-21$ time instants during 2nd oscillation cycle. (Measurement No57. The air flows from the right to the left.)

It should be noted that the beginning and end of the closing and opening phases of the glottis motion were not observed in the exactly identical times along the vocal folds model. This could emphasize 3D effects in the flow in the vocal tract.

The results evaluated from the PIV measurements are shown in Figures 5 and 6, where the airflow velocity and streamlines patterns, respectively, are presented, each during one vocal fold oscillation period. The denoted time instants exactly correspond to the sampling frequency of the glottal gap width as shown in Figure 4. The images of the vibrating vocal folds recorded in the same time instants are added to the right hand side of each airflow velocity and streamline patterns. A small circle on each image denotes the position of a maximum of the airflow velocity evaluated in each time instant. The maximum airflow velocities of about 90 m/s are observed near the vocal folds outlet in a maximum glottis opening (see the time instants $i=1$ and 11 in Figure 5 and $i=21$ in Figure 6). Mainly in the wider region of the channel modelling the epiglottis part of the vocal tract and situated on the left side from the model of the ventricular folds it is possible to see large vortices dimensions of that are comparable with the height (cross-section) of the channel (see, e.g. streamline patterns for $i=15-18$ in Figure 6). The vortices are disappearing quickly and in the narrowest part of the vocal tract model just before entering the model of the mouth the large vortices disappear and the flow is getting uniform (see, e.g. the images for the time instants $i=1-3$ and $i=10-11$). No flow structures resembling the Coanda effect [10] can be observed in this part of the vocal tract model.

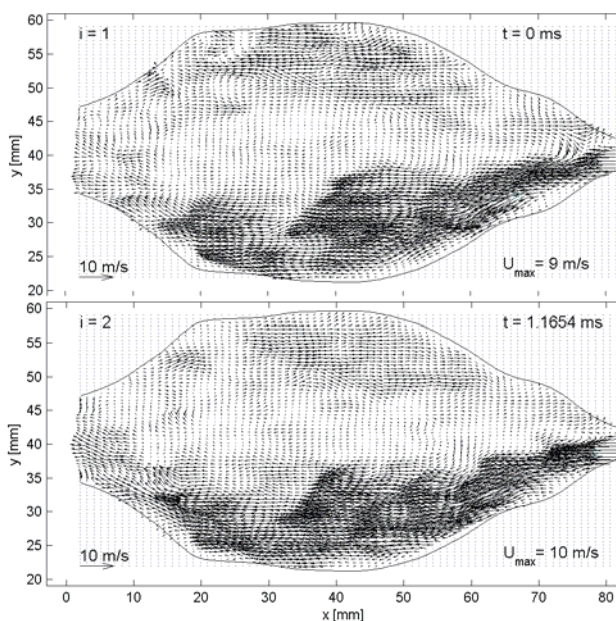


Figure 9: Airflow velocity patterns measured in 2 time instants in the outlet part of the vocal tract, in the model of the mouth cavity. (Measurement No 75 – $F_0=154$ Hz, $Q_{\text{mean}}=0.26$ l/s, $f_{\text{las}}=858$ Hz, $\Delta t=8$ μ s). (The air flows from the right to the left.)

An example of the flow field measured in the mouth part of the vocal tract model is shown in Figure 7 in 2 time instants ($i=1-2$). The flow velocities are here much lower than in the glottal part of the vocal tract model. Large eddies of a size comparable with the channel height are clearly noticeable in the airflow velocity patterns in the model of the mouth cavity. The airflow seems to be permanently attached to one wall of the channel, to the left side from the centerline, such flow-pattern resembles to the Coanda effect.

Conclusion

It is possible to see flow structures resembling large vortices with dimensions comparable with the channel cross-section above the ventricular folds. The vortices disappear in the narrowest epilaryngeal part of the vocal tract where the flow is uniform. Considerable 3D effects of the glottal flow were observed in the vocal tract near the vibrating vocal folds, especially for higher airflow rates. Large eddies of a size comparable with the channel height were observed in the model of the mouth cavity where the airflow was attached to one wall of the channel resembling a Coanda effect [10].

Acknowledgement. The research is supported by the Grant Agency of the Czech Republic by project No 101/08/115.

References

- [1] Titze IR.: Principles of voice production. Iowa City, IA: National Center for voice and Speech 2000
- [2] Scherer RC., Shinwari D., De Witt KJ., Zhang C., Kucinschi BR., Afjeh AA.: Intraglottal pressure profiles for a symmetric and oblique glottis with an divergence angle of 10 degrees. J. Acoust. Soc. Am. **109** (2001), 1616-1630
- [3] Hofmans GDJ., Groot G., Ranucci M., Graziani G., Hirschberg A.: Unsteady flow through in-vitro models of the glottis. J. Acoust. Soc. Am. **113** (2003), 1658-1675
- [4] Deverge M., Pelorson X., Vilain C., Lagree P., Chentouf F., Willems J., Hirschberg A.: Influence of collision on the flow through in-vitro rigid models of the vocal folds. J. Acoust. Soc. Am. **114** (2003), 3354-3362
- [5] Erath B., Plesniak M.: The occurrence of the Coanda effect in pulsatile flow through static models of the human vocal folds. Experim. Fluids **41** (2006), 735-748
- [6] Neubauer J., Zhang Z., Miraghaie R., Berry DA.: Coherent structures of the near field flow in a self-oscillating physical model of the vocal folds. J. Acoust. Soc. Am. **121** (2007), 1102-1118
- [7] Šidlof P., Horáček J.: Mathematical and physical modeling of flow-induced vibrations of human vocal folds. In *Flow Induced Vibration*, Zolotarev & Horáček eds., Institute of Thermomechanics, Prague 2008, pp. 141-146
- [8] Brücker Ch., Triep M., Mattheus W., Schwarze R.: Pulsating jet generated by a driven glottis-shaped Orifice. Int. Conf. on Jets, Wakes and Separated Flows, Sept.16-19, 2008, Technical University of Berlin, 8p.
- [9] Vampola T., Horáček J., Švec JG.: FE modeling of human vocal tract acoustics. Part I: Production of Czech vowels. Acta Acustica united with Acustica **94** (2008), 433-447
- [10] Tao Ch., Zhang Y., Hottinger G., Jiang. JJ.: Asymmetric airflow and vibration induced by Coanda effect in a symmetric model of the vocal folds. J. Acoust. Soc. Am. **122** (2007), 2270-2278